ISSN 1392 - 1207. MECHANIKA. 2013 Volume 19(3): 349-357

On different FE-based models to simulate cutting operation of Titanium alloy (Ti-6Al-4V)

Y. Zhang*, D. Umbrello, T. Mabrouki*, S. Rizzuti***, D. Nelias*, Y. Gong******

**Université de Lyon, CNRS, INSA-Lyon, LaMCoS, UMR5259, F69621, France, E-mail: zyc8910@yahoo.cn*

***University of Calabria, Department of Mechanical Engineering, 87036 Rende (CS), Italy, E-mail:* d.umbrello@unical.it

****Politecnico di Torino, DISPEA, 10129 Torino, Italy, E-mail: stefania.rizzuti@polito.it*

*****Northeastern University, School of Mechanical Engineering & Automation, Shenyang, 110819, China, E-mail: gongyd@mail.neu.edu.cn*

crossref http://dx.doi.org/10.5755/j01.mech.19.3.4656

1. Introduction

As it is known, finite element (FE) method provides precise information concerning variables like plastic strain, strain rate or stress evolutions during tool-workpiece interaction, which are difficult to measure experimentally. After the early FE model [1], many research works about metal cutting process have been performed. Wherein, Mabrouki et al. [2] studied the chip formation and cutting force for dry cutting with thermal physical coupled damage model, they also considered the grain microstructure in the cutting model [3]. Filice et al. [4] developed a wear model for the orthogonal cutting using uncoated carbide tools. Outeiro et al. [5] predicted the residual stresses in the cutting process, in particular. Finally, Umbrello et al. [6] incorporated the microstructure transformation for predicting residual stresses.

With these numerical methods, a general understanding of chip formation process can be improved. However, the effectiveness of these models depends, to a large extent, on how accurate are the models used to describe the metal cutting process and also the quality of the input data used in such models, especially when different commercial codes are used to develop the cutting model.

In recent years, researchers tried to find adequate FE-models and simulation parameters for different FE software and metal materials. Deshayes et al. [7] have carried out, based on a FE method comparison, a study dealing with the cutting of AISI4340 steel alloy with ADVANTEDGE and ABAQUS/EXPLICIT. Similar cutting simulations, with the two cited software, were also performed by Arrazola et al. [8] in the case of AISI4140. Soriano et al. [9] have also presented a comparison of 3D machining models developed under commercially available FE software ABAQUS/EXPLICIT, ADVANTEDGE and DEFORM3D for the machined material Inconel 718.

Considering all above, it is necessary to conduct a comparison study to evaluate the effectiveness of current predictive models not only regarding forces, temperature distribution, chip compression and morphology, but also parameters related with the integrity/quality of the machined surface, such as residual stress, etc.

2. Aim of study

Benchmark studies are commonly carried out in a manner that all conditions are kept equal for all the models of interest. Nevertheless, it has been proved [10] that for machining process it not possible to conduct a benchmark as usually done for the other manufacturing processes. In fact, it was shown that each model results to be properly predictive only if calibrated in the own simulation strategy. A specific combination of material and damage models furnishes good numerical results when these models are implemented in the same FE-code used for calibrating material constants [10]. This happens since mechanical theories, especially for damage models, implemented in FE-codes are different as well as are different the thermal models applied for describing the temperature and its evolution.

In this context, the aim of the study is to develop and calibrate two different simulation models and apply them to predict the most significant cutting parameters, comparing the different predictive capabilities. Thus, for each FE model the most appropriated combination of flow stress model, damage criterion and thermal model has been utilized. Obviously, it is worth pointing out that the proposed flow stress models, although dissimilar in their structure and for material constants, describe equivalent material behaviour. In such circumstances, the study is performed in the optimum conditions for the two different simulation models. In addition, it also permits to highlight the main problems related to current simulations supporting metal cutting researchers for understanding the cutting process and its influence on the material.

This paper is composed of three main parts: after a brief description concerning the material properties of Ti-alloy, the numerical model setups in ABAQUS/EXPLICIT (v6.7) and DEFORM/IMPLICIT-2D (v10.1) are described. Finally, the numerical and experimental results are detailed, discussed and overall conclusions are pointed out.

3. Material properties

The workpiece material selected for this study is the Titanium alloy Ti-6Al-4V, which has good specific strength, toughness and corrosion resistance making it attractive for aerospace applications, surgical implants, etc. Consequently, mechanical structure components for these applications have precise requirements in terms of physical, chemical properties [11] (Table 1), and thermo properties [12] (Fig. 1).

Table 1

Physical and chemical properties of Ti-6Al-4V [11]

Al, %	C, %	H, %	Fe, %	N, %	O, %	Ti, %	V, %	S, %	E, GPa	ν	ρ, kg/m^3	C_p, J/kg/°C	k, W/m/°C
5.5 - 6.8	≤ 0.08	≤ 0.015	≤ 0.4	≤ 0.3	≤ 0.2	87.7 - 91.0	3.5 - 4.5	< 0.05	110	0.3	4430	Fig. 1., a	Fig. 1., b

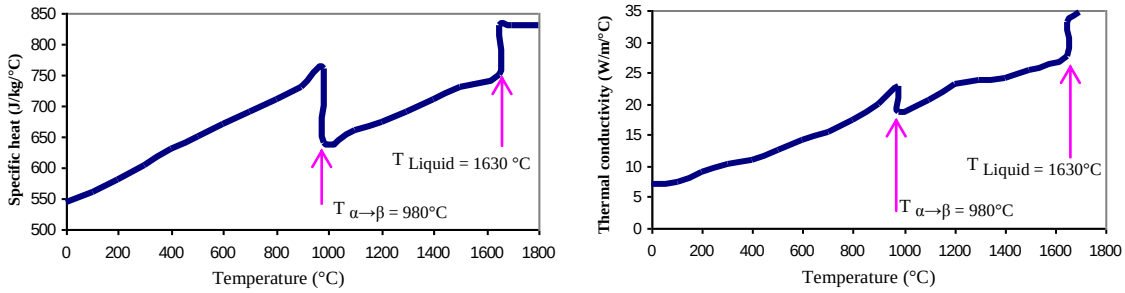

a b

Fig. 1 Physical properties of the Ti-6Al-4V alloy as a function of temperature: a) specific heat, C_p and *b*) thermal conductivity, k [12]

4. Finite element modelling

In order to build a common FE-model for chip formation process during orthogonal cutting process, ABAQUS/EXPLICIT-2D and DEFORM/IMPLICIT-2D software have been adopted.

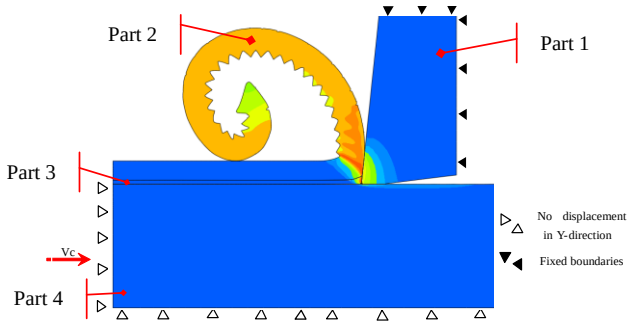

Fig. 2 Geometrical model and its boundary conditions

4.1. ABAQUS/EXPLICIT™: Model features

The software ABAQUS/EXPLICIT (V6.7) has been used to set up a FE-model in two-dimensions (2D) as presented in Fig. 2. To control the contact between tool and workpiece during cutting simulation, four parts are participated for the cutting model (Fig. 2) [13]. The workpiece is allowed to move with the cutting speed, while the tool is fixed on its top and right sides.

4.1.1. Material constitutive model

Concerning the material behavior of Ti-6Al-4V, the Johnson-Cook (J-C) constitutive model [14] is implemented in ABAQUS and is expressed by the following equation of the equivalent stress:

$$\bar{\sigma} = \left[A + B\left(\bar{\varepsilon}\right)^n\right] \cdot \left[1 + C\, ln\left(\dot{\bar{\varepsilon}}/\dot{\bar{\varepsilon}}_0\right)\right] \cdot \left[1 - \left(\frac{\theta_w - \theta_0}{\theta_m - \theta_0}\right)^m\right]. \quad (1)$$

The values of coefficients A, B, C, n and m for the Ti-6Al-4V alloy are reported in Table 2 from the work of [13].

Table 2

Thermo-physical parameters for the ABAQUS FE model

Parameters			Value
Material	Plastic Johnson-Cook Law	A, MPa	1098
		B, MPa	1092
		n	0.93
		C	0.014
		m	1.1
	Proprieties	Workpiece	Tool (P20)
	Density ρ, kg m^{-3}	4430	15700
	Elasticity E, GPa	210	705
	Poisson's ratio ν	0.33	0.23
	Inelastic heat fraction β	0.9	×
	Conductivity k, W m^{-1} °C^{-1}	See Fig. 1	24
	Specific heat c, J Kg^{-1} °C^{-1}	See Fig. 1	178
	Expansion α_d, µm m^{-1} °C^{-1}	9	5
	T_{melt}, °C	1630	×
	T_{room}, °C	20	20

4.1.2. Chip formation criterion

In the present model, the adopted numerical methodology is based on the fracture energy as an intrinsic material parameter for controlling damage evolution criterion after damage initiation.

Damage initiation

The strain cumulative damage law is employed for the damage initiation:

$$\omega = \sum \frac{\Delta\bar{\varepsilon}}{\bar{\varepsilon}_{0i}}, \quad (2)$$

where $\Delta\bar{\varepsilon}$ is the equivalent plastic strain increment in one loading increment and $\bar{\varepsilon}_{0i}$ is the equivalent plastic strain is used for determining the damage initiation:

$$\bar{\varepsilon}_{0i} = \left[D_1 + D_2\, exp\left(D_3\sigma^*\right)\right]\left[1 + D_4\, ln\,\dot{\bar{\varepsilon}}^*\right]\left[1 + D_5 T^*\right]. \quad (3)$$

The constant parameters for Eq. (3) are from [13]. Damage initiation is assumed to be activated when $\omega = 1$.

Damage evolution

The evolution of damage is based on the concept of the Hillerborg's fracture energy [15, 16], which is presented as a stress-displacement response after damage initiation:

$$G_f = \int_{\bar{\varepsilon}_0^{pl}}^{\bar{\varepsilon}_f^{pl}} L\sigma_Y d\bar{\varepsilon}^{pl} = \int_0^{\bar{u}_f^{pl}} \sigma_Y d\bar{u}^{pl} \,, \tag{4}$$

where L is the characteristic length presented by the square root of the integration point element area. The linear and exponential damage evolutions are adopted part 3 and part 2 respectively [13]. For plane strain condition, the adopted G_f can be deduced by:

$$G_f = K_C^2 \left(1-\nu^2\right) / E \,, \tag{5}$$

where K_C is the fracture toughness [11].

Moreover, the classic Zorev's [17] stick-slip friction model is implemented to simulate frictional contact between chip and tool with a constant friction coefficient [13]. Finally, the thermo-physical properties of both cutting tool and workpiece are given in Table 2. The contact and damage data can be obtained from [13].

4.2. DEFORM/IMPLICIT: Model features

Parallel to the cutting simulations performed with ABAQUS, other FE based simulations were carried out using DEFORM2D, which makes use of an implicit Lagrange formulation. A plane strain coupled thermo-mechanical analysis is performed in orthogonal cutting conditions. The workpiece is meshed with isoparametric quadrilateral elements and modelled as elastic-visco-plastic, while the tool is modelled as rigid.

The material behaviour for Ti-6Al-4V is modelled with the flow stress developed by Scientific Forming Technologies Corporation (SFTC) based on the works in [18, 19]. It is important to highlight that such flow stress exhibit similar behaviour for Ti-6Al-4V alloy of the J-C model implemented in ABAQUS.

4.2.1. Constitutive equation

An elastic-visco-plastic material model with Von Mises yield criterion and associated flow rule is used. In the deformation zone, the following equation is given:

$$\dot{\varepsilon}_{ij} = \frac{3}{2}\frac{\dot{\bar{\varepsilon}}}{\bar{\sigma}}\sigma'_{ij} \,, \tag{6}$$

where: $\dot{\varepsilon}_{ij}$ are strain rate components; σ'_{ij} is the deviatoric stress and $\bar{\sigma}$ and $\dot{\bar{\varepsilon}}$ are effective stress and strain rate.

4.2.2. Chip formation criterion

The chip segmentation is a consequence of the fracture process that takes place during chip formation. In this research, Cockroft and Latham's fracture criterion (CLFC) [20] (Eq. (7)) were adopted to present the effect of the stress on the chip segmentation:

$$\int_0^{\bar{\varepsilon}_f} \sigma_1 d\bar{\varepsilon} = C \,, \tag{7}$$

Where: ε_f is the effective strain; σ_1 principal stress and C the material constant representing resistance to failure (sometimes called "damage value"). CLFC means that when the integral of the left term (applied state) in Eq. (7) reaches the value of C (material state), the fracture occurs and the chip segmentation starts. Usually, the adequate C value is determined by numerical calibration on available experimental data. In this work, C is set equal to 240 MPa as found by SFTC through the above mentioned calibration.

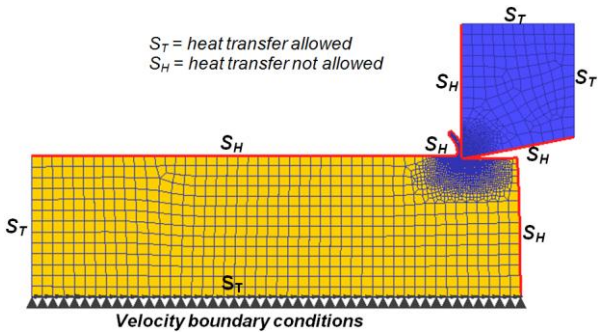

Fig. 3 2D numerical model set up (DEFORM /IMPLICIT)

In Fig. 3, the mechanical and thermal boundary conditions of the 2D FE model are schematically shown. As far as friction modeling is concerned, a simple model based on the constant shear hypothesis is implemented with the shear factor kept at m = 0.6, considering as dominant the phenomena appearing in the sticking zone, in which this model is effective.

This value is chosen on the basis of an iterative procedure aimed at reducing the errors on the predictions of cutting forces, chip morphology parameters and temperature distribution as well as thermal steady-state along primary and secondary shear zones.

5. Experimental design

To evaluate the robustness of the two simulation models, several numerical tests are taken into account. In particular, the numerical values obtained by means of FE simulation, in terms of cutting force (F_c), thrust force (F_t), cheap peak (h_1), chip valley (h_2), chip pitch (L_1), chip compression ratio (CCR), maximum temperature on workpiece (T_W) and maximum temperature over the tool rake surface (T_T), are considered and compared with those experimentally available in literature [10, 18, 21, 22]. Furthermore, numerical residual stress profiles in circumferential direction are numerically extracted from the machined surface and sub-surface and compared with those experimentally measured by X-Ray Diffraction (XRD) technique [10]. Schematically speaking, the available experimental data are divided into four groups.

The first group is mainly focused on studying the physical phenomenon accompanying cutting process with positive rake angle of the cutting tool [18]. The second group concerns the cutting with negative rake angle [21], and the third group aims to investigate the effect of the tool wear on the residual stress distribution after machining [22]. Finally, the fourth group focuses on studying the influence of the V_C variation on the residual stress evolution considering a constant tool flank wear [10]. The cutting conditions are summarized in Table 3.

Table 3

Process parameters employed in the study

Cutting parameters		Group I [18]	Group II [21]	Group III [22]		Group IV [10]	
				III-1	III-2	IV-1	IV-2
Cutting speed *Vc*, m/min		120	180	320	320	55	90
Uncut chip thickness, mm		0.127	0.1	0.1	0.1	0.15	0.15
Depth of cut, mm		2.54	2	1	1	4	4
Cutting edge radius, μm		30	20	sharp	sharp	30	30
Rake angle, deg		15	-4	5	5	6	6
Clearance angle, deg		6	7	8	8	7	7
Flank wear, mm		-	-	0.03	0.2	0.14	0.14
Experimental Results							
Force	Cutting force F_c , N	559	548	-	-	748	
	Thrust force F_t , N	-	-	-	-	612	
Chip morphology	Chip peak h_1, μm	165	131	-	-	227	
	Chip valley h_2, μm	46	62	-	-	117	
	Chip pitch L_1, μm	140	100	-	-	161	
	Chip compression ratio: CCR	1.30	1.31	-	-	1.51	

6. Results and discussions

6.1. Cutting force evolution, chip morphology and temperature

Table 4 shows the computed results based on both ABAQUS and DEFORM simulations as far as cutting forces, chip morphology and temperature are regarded. Results concerning principal cutting force allow establishing that the two codes allow a good prediction regarding experimental ones although lowest errors can be obtained by using ABAQUS. In contrast, DEFORM allows to better describe the evolution of thrust forces, even if it is possible to compare the numerical values with only one experimental evidence (Group IV). Furthermore, DEFORM permits to better describe the evolution of both F_c and F_t instead of ABAQUS, since with increasing of the V_C, both the cutting forces decrease (Groups I and II). It is worth pointing out that this well-known behaviour is not observed neither from DEFORM as well as from ABAQUS when Group 4 is considered. In fact, both the FE codes exhibit higher cutting forces when V_C rises.

Chip morphology is analysed in terms of chip segment shape (valley, pick and pitch), as shown in Fig. 4. Numerical results are compared with experimental ones for groups I, II and IV (V_C = 90 m/min), while the simulation results from group III and the other case of Group IV can be used for qualitative comparison. Analyzing the errors obtained in the predictions of the chip morphology (Table 4), it is possible to state that from a numerical point of view, ABAQUS provided the lowest errors in most of the cases.

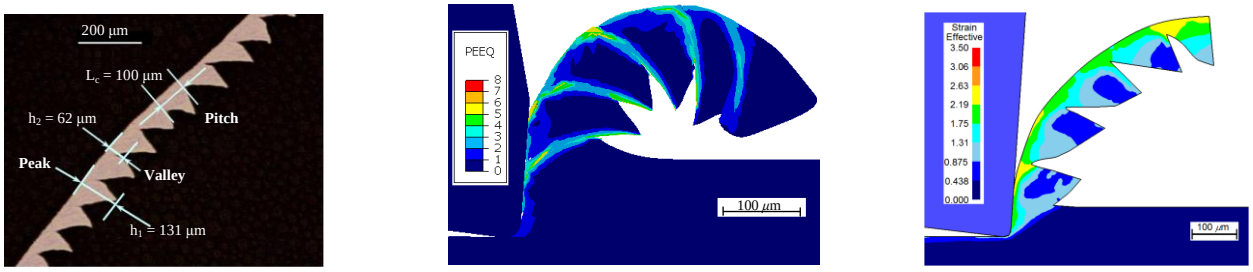

a b c

Fig. 4 Chip morphology obtained at V_C = 180 m/min, f = 0.1 mm/rev: a) Experimental chip [21]; Equivalent plastic strain computed with, b) ABAQUS/EXPLICIT and c) DEFORM/IMPLICIT

Regarding the chip formation process, it is worth underlining that in ABAQUS the chip segmentation is the result of a thermal softening state coupled with damage degradation. Moreover, the element deletion is available only in the sacrificial zone, while the other part, which is not deleted, becomes part of the chip. In DEFORM software, the chip formation is obtained by implementing Cockroft and Latham's criterion, thus allowing to describe the effect of tensile stress on the chip segmentation during orthogonal cutting. In addition, in DEFORM, the element deletion feature is also applied in these numerical simulations to better describe the chip fracture instead of the remeshing methodology. Finally, for all the investigated cases, both the maximum temperature range on both tool and workpiece are collected. As it can be observed, the results are almost similar although those found in DEFORM exhibits always higher values of about 50 - 100°C compared to those revealed in ABAQUS. Such discrepancy is related to the thermal models used in the cited FE codes as better illustrate in the next paragraph on which the influence of tool wear on thermal field and temperature distribution is investigated.

Table 4

Numerical effects obtained after the sensitivity analysis with two FE – Codes

	Simulation Test		Cutting force		Chip morphology parameters				Work-	Tool
			F_c	F_t	h_1	h_2	L_1	CCR	θ_{WT}	θ_{TT}
ABAQUS	GI_Vc_120		541.3	39.0	161.5	48.0	133.0	1.27	591-689	486-631
	Error with experiment, %		-3.17	-	-2.12	4.35	-5	-2.12	-	-
	GII_Vc_180		580.0	164.5	132.0	77.0	96	1.32	754-919	462-611
	Error with experiment, %		5.8	-	0.76	24.19	-4	0.76	-	-
	GIII_Vc _320	Wear_0.03	166.5	21.0	131.2	34.0	96.0	1.31	631-693	514-580
		Wear_0.2	186.9	40.4	131.7	31.2	96.0	1.32	629-699	541-603
	GIV_V_B _0.14	Vc_55	947	208	186.9	69	136.1	1.24	466-523	263-321
		Error with experiment, %	30	-66	-17.6	-41.0	-15.5	-17.44	-	-
		Vc_ 90	1022	305	186.9	51.4	136.1	1.25	546-585	294-379
DEFORM	GI_Vc_120		508.9	305.4	152	42	133	1.20	678-781	621-707
	Error with experiment, %		-8.96	-	-7.88	-8.70	-5.00	-7.69	-	-
	GII_Vc_180		501.1	270.9	155.5	47.8	121.0	1.55	820-934	672-766
	Error with experiment, %		-8.56	-	18.70	-22.90	21	18.32	-	-
	GIII_Vc _320	Wear_0.03	228	101	157	34.1	214.5	1.57	805-918	793-903
		Wear_0.2	267	111	190.5	54	221.5	1.905	819-933	817-932
	GIV_V_B _0.14	Vc_55	844	380	213	55	176	1.42	570-725	459-580
		Error with experiment, %	12.8	-37.9	-6	-50	9.3	-5.9	-	-
		Vc_ 90	876	392	189	69	157	1.26	584-750	504-595

F_c, N: Cutting force. F_t, N: Thrust force. CCR: Chip compression ratio.
h_1, µm: Chip peak. h_2, µm: Chip valley. L_1, µm: chip pitch.
θ_{WT}, °C: Maximum temperature on workpiece θ_{TT}, °C: Maximum temperature over tool rake surface.

6.2. Temperature distribution due to tool wear

Two numerical comparisons were done in order to highlight the evolution of different outputs computed by ABAQUS and DEFORM software: (i) temperatures comparison on machined surface and subsurface near the tool tip for different flank wear; (ii) Temperatures distribution along the primary and secondary shear zones and their maximum values.

To analyze the influence of tool wear on temperature distribution beneath the machined surface, the flank wear size of cutting tool is considered as an initial state and kept constant during the cutting simulation. The tools' geometry shapes with flank wear are illustrated in Fig. 5.

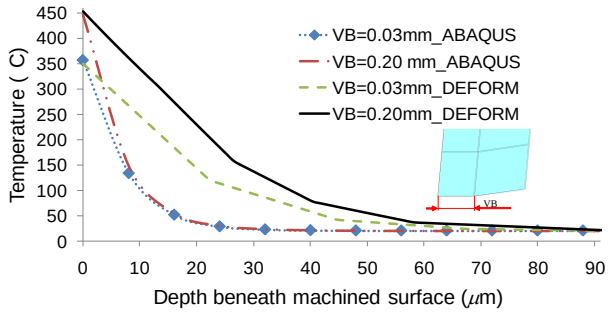

Fig. 5 Temperature distribution beneath the machined surface

Fig. 5 shows that both DEFORM and ABAQUS predict similar temperature values on the machined surface. Furthermore, for a given code numerical results present a temperature gradient about 90°C for the two flank wear lengths at the generated surface. Therefore, both DEFORM and ABAQUS take into account the heat generated along the flank face/workpiece interface due to modelled flank wear. In contrast, there is some discrepancy in temperature prediction below the machined surface (Fig. 5) since for both modelled tool flank wears, DEFORM shows higher temperature than ABAQUS. The reason is related to the different heat global coefficient and interface thermal model adopted and implemented in the two used software. Moreover, the difference is also due to the different description of the movements.

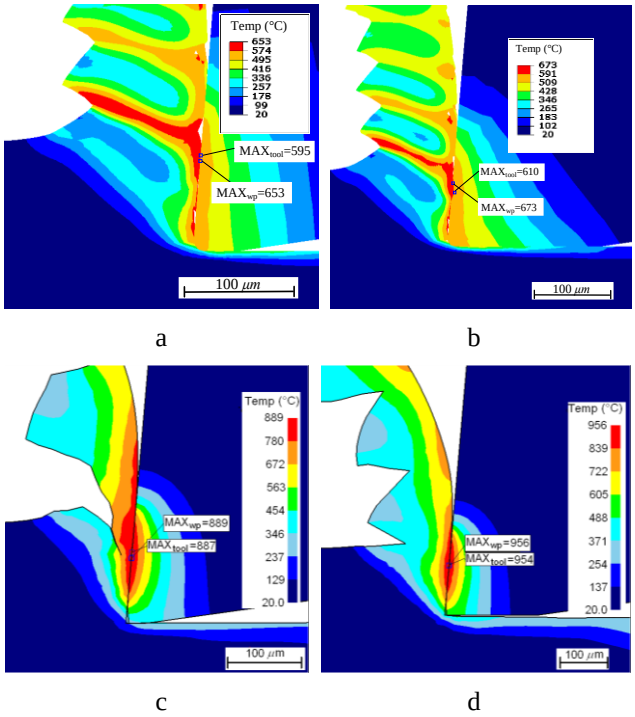

Fig. 6 Temperature distribution at the tool-chip-workpiece interfaces: a) VB = 0.03 mm; b) VB = 0.20 mm based on ABAQUS; c) VB = 0.03 mm; d) VB = = 0.20 mm based on DEFROM

In addition, the temperature distribution in the whole cutting model is presented in Fig. 6. It can be noted

that there is a disagreement between ABAQUS and DEFORM. Also, it is underlined that a non-concordance in the chip morphologies. Indeed, the chip segmentation morphology obtained by ABAQUS is the result of a thermal softening state coupled with damage degradation. The temperature given by DEFORM modelling is higher at the secondary shear zone and this is due to the fact that the contact is considered as perfect at tool-chip interface.

Besides both DEFORM and ABAQUS show a maximum temperature increase when tool with higher flank wear is used. Except these similarities between the two software, DEFORM shows higher maximum temperatures in both tool and chip. The reason is once again related to the different formulation, interface thermal model and heat global exchange coefficient at the tool/chip interface (the low value of heat exchange coefficient at the tool/chip interface directly leads to the temperature discontinuity at the rake face for ABAQUS, which is assumed that the non-perfect contact condition is considered between tool chip interface under simulation test).

6.3. Residual stress distribution considering tool wear

To consider the effect of successive cutting sequences on residual stress distribution, the physical state from the first cut is saved and used as initial condition for the second one. Other cutting conditions of the second cut are the same as those of the first one. In order to predict residual stress based on ABAQUS software, three unloading steps were implemented at the end of each cut in this study:

1. release of the cutting forces;
2. release of the clamping forces;
3. release of the workpiece to the room temperature.

After external force release and cooling down to room temperature, the final residual stress distribution on the workpiece is shown in Fig. 7.

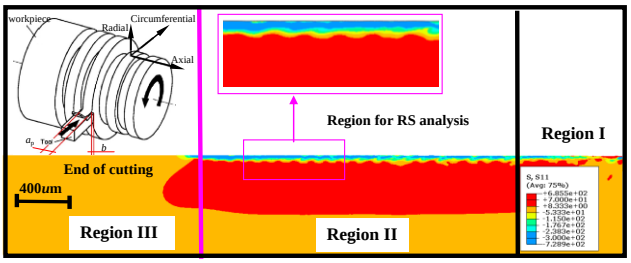

Fig. 7 Residual stress distribution on the workpiece

The stresses in Region II are selected to evaluate the residual stresses, and the predicted residual stresses should be also averaged over the same volume and the mean value should be taken. The oscillated residual stresses caused by the segmented chip are observed on the machined surface, which present the microstructure of the machined surface. It should be mentioned that the residual stress is extracted from element integration point. Consequently, the stress on the machined surface is located at the centre of the first layer element (4 μm below the machined surface), and the stresses are averaged along 2-3 mm in the circumferential direction after their calculation in element integration points. Vice versa, as far as DEFORM procedure since an automatic method for residual stress collection is not yet implemented in SFTC-DEFORM-2D V.10, the following procedure was employed:

1. for several time steps, the tool was released from the machined surface (unloading phase) and the workpiece was cooled down to the room temperature;
2. residual stress profiles at several locations (coincident to Region II, Fig. 7.) of the machined surface were collected and the average values were calculated, as described in the work of Liu and Guo [23].

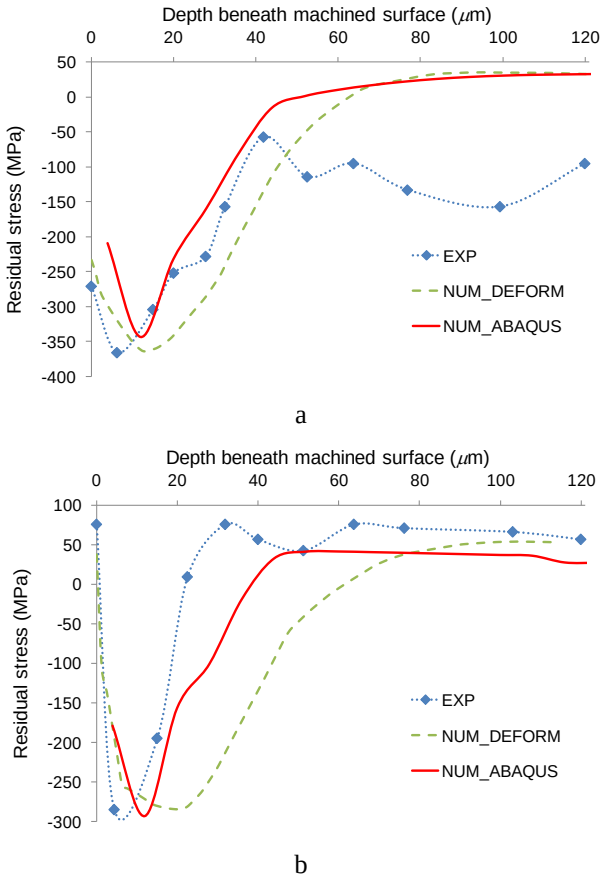

Fig. 8 Effect of the flank wear lengths on residual stress profile with V_C = 320 m/min: a) VB = 0.03 mm; b) VB = 0.2 mm

Fig. 8 shows the effect of flank wear length on circumferential residual stress distribution beneath the newly machined surface. As general trends, both the software highlight that when the flank wear was increased from 0.03 to 0.2 mm, the surface residual stress towards the tensile region. This is due to the higher magnitude of temperature generated along flank face/workpiece interface.

Moreover, both DEFORM and ABAQUS show that the maximum compressive residual stress as well as the beneficial depth decreases with increasing of flank wear. In addition, the distance where maximum compressive residual stress is located seems to be not affected by flank wear. However, both the software show some gap between experiments and simulations when considering the influence of first cut. The reason of such discrepancy should be related to firstly the material flow stresses used in both ABAQUS and DEFORM which are not suitable for describing pertinently material states. Secondly, It is worth pointing out that in both computations, the residual stresses due to phase transformation were neglected and, especially

in the case of DEFORM (temperature near to phase transformation effect), such assumption is not properly corrected.

6.4. Cutting speed effect on residual stress distribution considering a fixed tool wear

To study the influence on circumferential residual stress distribution on the machined surface, different cutting speeds varying from V_C = 55 m/min to V_C = 90 m/min with constant flank wear are adopted in Fig. 9.

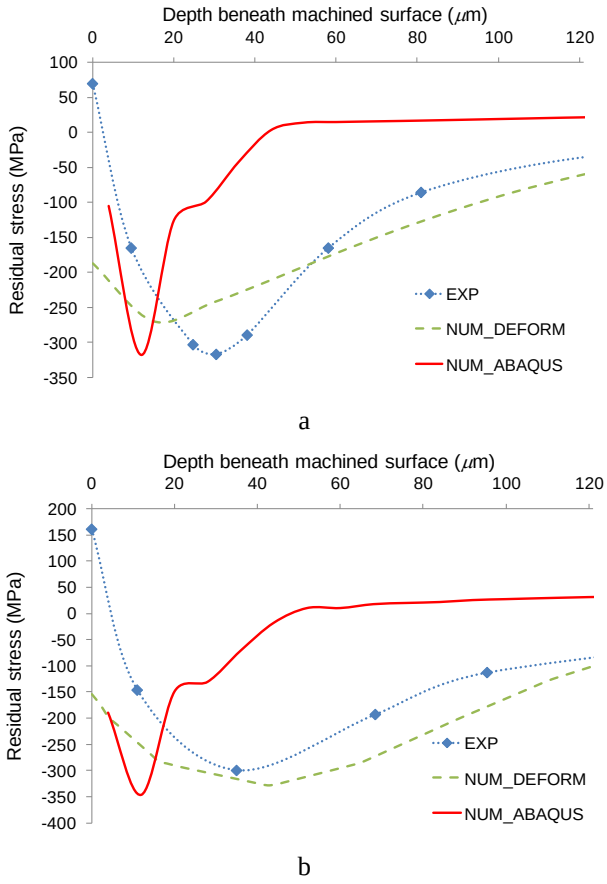

Fig. 9 Effect of the V_C on residual stress profile with constant VB = 0.15 mm: a) V_C = 55 m/min; b) V_C = 90 m/min

It can be noted that, the distribution of the compressive RS computed by ABAQUS is still mainly localized within 60 µm, while the simulation result from DEFORM extends to 200 µm, which shows an acceptable numerical RS prediction compared to ABAQUS. However, both two codes illustrate that the maximum compressive RS as well as the beneficial depth increases with increasing of the cutting speed, which is in contrast with the experimental facts. It implies that the contact thermal properties between tool/machined surface still need to improve for both codes mentioned above.

6.5. Effectiveness and Robustness of FE codes: comparison and overall

Taking into account what it is discussed in the previous paragraphs and in order to complete the assessment of the two described simulation strategies, it is useful at this point to draw an overall comparison between the two used codes for cutting modeling. In order to perform detailed simulations and precise control for the mesh and the boundary conditions, then the software package ABAQUS seems to be adequate. However, if an efficient, easy to setup machining simulation is needed, and then the software package DEFORM seems to be satisfactory. This package allows quick setup of simulations and provides the built in modules for material library, tool and workpiece geometries and process parameters.

7. Conclusions

In this study, a comparison of four groups of simulations performed with two different 2D FE models is presented in the case of Ti-6Al-4V alloy cutting. The computed results were compared with experimental ones. Some observations concerning the results obtained based on the using of ABAQUS and DEFORM can be pointed following:

1. The serrated chip formation can be modelled using the mentioned two codes with appropriate material and damage models.
2. The temperature distribution at the tool-chip-workpiece interfaces displays that the segmentation is the result of a thermal softening state or/and the coexisting fracture phenomenon, among other phenomena.
3. The simulation results of temperature and residual stress show the similar tendency for two kinds of models, even though there is some gap between them due to the optimal conditions for each of them (material laws, damage criteria, etc.
4. Potentially, these two simulated models can be exploited to perform other numerical comparisons with both commercial and in-house codes.

Acknowledgments

The authors of LaMCoS laboratory would like to acknowledge the financial support of China Scholarship Council (CSC), and National Natural Science Foundation of China (Microscale grinding and micro milling-grinding compound machining process, support No. 52075064).

References

1. **Shirakashi, T.**; **Usui, E.** 1974. Simulation analysis of orthogonal metal cutting mechanism, In Proceedings of the first international conference on production engineering, Part I: 535-540.
2. **Mabrouki, T.; Girardin, T.; Asad. M.; Rigal, J.F.** 2008. Numerical and experimental study of dry cutting for an aeronautic aluminium alloy (A2024-T351), Int. J. Mach. Tool. Manu. 48(11): 1187-1197. http://dx.doi.org/10.1016/j.ijmachtools.2008.03.013.
3. **Zhang, Y.; Mabrouki, T.; Nelias, D.; Courbon, C.; Rech, J.; Gong, Y.** 2012. Cutting simulation capabilities based on crystal plasticity theory and discrete cohesive elements, Journal of Materials Processing Technology 212(4): 936- 953. http://dx.doi.org/10.1016/j.jmatprotec.2011.12.001.
4. **Filice, L.; Micari, F.; Settineri L.; Umbrello, D.** 2007. Wear modelling in mild steel orthogonal cutting when using uncoated carbide tools, Wear

262(5-6): 545-554.
http://dx.doi.org/10.1016/j.wear.2006.06.022.

5. **Outeiro, J.C.; Umbrello, D.; M´Saoubi, R.** 2006. Experimental and numerical modeling of the residual stresses induced in orthogonal cutting of AISI 316L Steel, Int. J. Mach. Tool. Manu. 46: 1786-1794. http://dx.doi.org/10.1016/j.ijmachtools.2005.11.013.
6. **Umbrello, D.; Outeiro, J.C.; M'Saoubi, R.; Jayal, A.D.; Jawahir, I. S.** 2010. A numerical model incorporating the microstructure alteration for predicting residual stresses in hard machining of AISI 52100 Steel, Annals of the CIRP 59(1): 113-116. http://dx.doi.org/10.1016/j.cirp.2010.03.061.
7. **Deshayes, L.; Mabrouki, T.; Ivester, R.; Rigal, J. F.** 2004. Serrated chip morphology and comparison with finite elements simulation, In Proceedings of 2004 ASME International Mechanical Engineering Congress and Exposition American Society of Mechanical Engineers, Anaheim, California USA, 815-824.
8. **Arrazola, P.J.; Ugarte, D.; Montoya, J.; Villar, A.; Marya, S.** 2005. Finite element modeling of chip formation process with ABAQUS/EXPLICITTM 6.3. In Proceeding of VIII International Conference on Computational Plasticity, CIMNE, Barcelona.
9. **Soriano, J.; Llanos, I.; Ozel, T.; Arrazola, P.J.** 2009. Comparison of 3D finite element models for chip formation process developed under different FE software, In Proceeding of 12th CIRP Conference on Modelling of Machining Operations, Donostia-San Sebastián, Spain, May 7-8.
10. **Outeiro, J.C.; Jawahir, I.S.; M'Saoubi, R.; Umbrello, D.; Jayal, A. D.** 2011. Benchmark Report on "Evaluation of Predictive Models", In Proceeding of CIRP – CWG on Surface Integrity and Functional Performance of Components, Paris, France, January 26th.
11. **Matweb.** 2010. Material property data of Ti-6Al-4V, available from http://www.matweb.com.
12. **Mills, K.C.** 2002. Recommended values of thermo physical properties for selected commercial alloys (Woodhead Publishing Limited, Abington Hall, Abington).
13. **Zhang, Y.C.; Mabrouki, T.; Nelias, D.; Gong, Y.D.** 2011. Chip formation in orthogonal cutting considering interface limiting shear stress and damage evolution based on fracture energy approach. Finite Elements in Analysis and Design 47: 850-863. http://dx.doi.org/10.1016/j.finel.2011.02.016.
14. **Johnson, G.R.; Cook, W.H.** 1983. A constitutive model and data for metals subject to large strains, high strain rates and high temperatures, In Proceedings of the 7th international symposium on ballistics, the Hague: 31-48.
15. **Hillerborg, A.; Modéer, M.; Petersson, P.E.** 1976. Analysis of crack formation and crack growth in concrete by means of fracture mechanics and finite elements, Cement Concrete Res. 6: 773-782. http://dx.doi.org/10.1016/0008-8846(76)90007-7.
16. **ABAQUS** analysis user's manual Version 6.7, Dassault Systems, 2010.
17. **Zorev, N.N.** 1963. Inter-relationship between shear processes occurring along tool face and shear plane in metal cutting, Int. Resea. Prod. Engi., ASME : 42-49.
18. **Umbrello, D.** 2008. Finite element simulation of conventional and high speed machining of Ti-6Al-4V alloy, J. Mater. Process. Tech. 196(1-3): 79-87. http://dx.doi.org/10.1016/j.jmatprotec.2007.05.007.
19. **DEFORM** User's Manual version 10.0.2, Scientific Forming Technologies Corporation, 2010.
20. **Cockcroft, M.G.; Latham, D.J.** 1968. Ductility and workability of metals, J. Inst. Metals. 96: 33-39.
21. **Calamaz, M.; Coupard, D.; Girot, F.** 2008. A new material model for 2D numerical simulation of serrated chip formation when machining titanium alloy Ti-6Al-4V, Int. J. Mach. Tool. Manu. 48(3-4): 275-288. http://dx.doi.org/10.1016/j.ijmachtools.2007.10.014.
22. **Chen, L.; El-Wardany, T.I.; Harris, W.C.** 2004. Modelling the effects of flank wear land and chip formation on residual stresses, CIRP Ann. – Mfg Technol. 53(1): 95-98.
23. **Liu, C.R.; Guo, Y.B.** 2000. Finite element analysis of the effect of sequential cuts and tool-chip friction on residual stresses in a machined layer, Int. J. Mech. Sci. 42(6): 1069-1086. http://dx.doi.org/10.1016/S0020-7403(99)00042-9.

Y. Zhang, D. Umbrello, T. Mabrouki, S. Rizzuti,
D. Nelias, Y. Gong

SKIRTINGŲ BAIGTINIŲ ELEMENTŲ MODELIŲ TAIKYMAS TITANO LYDINIO TI-6AL-4V PJOVIMO OPERACIJOMS

R e z i u m ė

Taikant baigtinių elementų modelius pjovimo operacijoms kyla didelė painiava dėl netiesiškų ir multifizikinių ryšių. Nepaisant to, nėra nusistovėjusio standarto pjovimo modeliams, sukurtiems skirtinga programine įranga, palyginti. Šiame darbe nagrinėjamos įvairios galimybės titano lydinio Ti-6Al-4V ortogonalaus pjovimo operacijas modeliuoti naudojantis dviem komerciniais paketais: ABAQUS ir DEFORM. Siekiama parodyti, kaip nagrinėjamas optimalus baigtinių elementų skaitinis priartėjimas gali veikti sutarimus ar prieštaravimus vertinant abiem paketais gautus rezultatus. Norint perduoti lyginamuosius rezultatus abiem atvejais buvo laikomasi panašių geometrinių ir pjovimo sąlygų. Pristatyta multifizikinė drožlės formavimosi, pjovimo jėgų, temperatūros kitimo ir paviršiaus integralumo įtakos samprata. Be to, siekiant išsamiau panagrinėti skaitines prielaidas, skaitiniai rezultatai palyginti su eksperimentiniais, o modeliavimo uždaviniai buvo skirti proceso inovacijoms panaudoti ir palaikyti.

Y. Zhang, D. Umbrello, T. Mabrouki, S. Rizzuti,
D. Nelias, Y. Gong

ON DIFFERENT FE-BASED MODELS TO SIMULATE CUTTING OPERATION OF TITANIUM ALLOY (TI-6AL-4V)

S u m m a r y

Finite element based models for cutting operation present outstanding complexities due to their nonlinear and multi-physics coupling. Nevertheless, there is no uniform standard for the comparison between cutting simulation models based on different software. The present work deals with various methodologies to simulate orthogonal cutting operation for Ti-6Al-4V Titanium alloy inside two commercial codes: ABAQUS and DEFORM. The aim is to show how considered optimal FE numerical approaches can imply agreements or disparities in outputs between the two pre-cited codes. In order to carry out a comparative study between the two codes, similar conditions concerning geometrical models and cutting parameters were adopted. A multi-physic comprehension related to chip formation, cutting forces, temperature evolutions, and surface integrity was presented. Moreover, the numerical results were compared with experimental ones for a deeper discussion on numerical predictions, and problems with current simulation were addressed to improve and support process innovations.

Keywords: Cutting simulation, FE Models, Effectiveness, Ti-6Al-4V.

Received December 06, 2011
Accepted May 15, 2013